ACS APPLIED MATERIALS & INTERFACES

Research Article

www.acsami.org

Surface-Assisted Unidirectional Orientation of ZnO Nanorods Hybridized with Nematic Liquid Crystals

Shoichi Kubo,*[,†] Rei Taguchi,[†] Shingo Hadano,[‡] Mamiko Narita,[§] Osamu Watanabe,[§] Tomokazu Iyoda,[∥] and Masaru Nakagawa[†]

[†]Institute of Multidisciplinary Research for Advanced Materials, Tohoku University, 2-1-1 Katahira, Aoba-ku, Sendai 980-8577, Japan

[‡]Department of Applied Science, Kochi University, 2-5-1 Akebono-cho, Kochi 780-8520, Japan

[§]Toyota Central R&D Labs., 41-1 Yokomichi, Nagakute, Aichi 480-1192, Japan

[∥]Chemical Resources Laboratory, Tokyo Institute of Technology, 4259 Nagatsuta, Midori-ku, Yokohama 226-8503, Japan

Supporting Information

ABSTRACT: Inorganic semiconductor nanorods are regarded as the primary components of optical and electrical nanoscale devices. In this paper, we demonstrate the unidirectional alignment of monolayered and dispersed ZnO nanorods on a rubbed polyimide alignment layer, which was achieved by a conventional liquid crystal alignment technique. The outermost surfaces of the ZnO nanorods (average diameter 7 nm; length 50 nm) were modified by polymerization initiator moieties, and nematic liquid crystalline (LC) methacrylate polymers were grown by atom transfer radical polymerization. By regulating the densities of the polymerization initiator moieties, we successfully hybridized LC-polymer-grafted ZnO nanorods and small nematic LC molecules. The LC-polymer-modified ZnO nanorods were hierarchically aligned on the substrate via cooperative molecular interactions among the liquid crystal mesogens, which induced molecular orientation on the rubbed polyimide alignment layer.

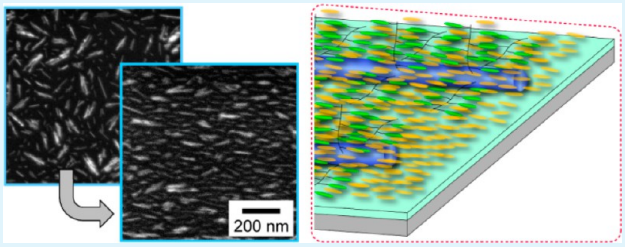

KEYWORDS: *inorganic nanorods, hybrid materials, nematic liquid crystals, polymer graft, cooperative molecular interaction*

1. INTRODUCTION

Inorganic semiconductor nanorods are regarded as the primary components of optical devices based on anisotropic photoluminescence[1−3] and advanced transistors and piezoelectric devices in nanoelectronics.[4−6] To effectively utilize the fascinating intrinsic properties of these structures, individual nanorods must be separately integrated onto solid substrates in an ordered manner. To date, the anisotropic optical properties of nanorods have been studied by diluting the nanorods in liquid crystals,[1] assembling them over a small area on a substrate,[2] and investigating them as single entities.[3] The electric properties of nanorods have been investigated by chance connection of single nanorods to two electrode terminals.[4−6] However, until current methods have been sufficiently improved for detailed studies of nanorods, the development of sophisticated nanorod-based devices is difficult. To date, a variety of nanorods, including ZnO,[7−16] ZnS,[17] TiO_2,[18,19] Ta_2O_5,[20] and Si,[21] have been vertically aligned on substrates by metal organic chemical vapor deposition,[7,12,17] hydrothermal methods,[11,18,19] chemical solution growth,[8−10] pulsed laser deposition,[13] and surfactant-assisted sol−gel processes.[14] Alternatively, presynthesized individual nanorods can be assembled onto the substrate. Electric fields,[22−25] self-assembling,[2,26−29] and selective incorporation into microphase-separated block copolymers[30] can achieve horizontally anisotropic alignment of nanorods on substrate surfaces. However, a more sophisticated approach that aligns the nanorods over a large area has not yet been developed.

Anisotropic fluid liquid crystals can potentially encourage nanorod alignment.[1,31,32] Indeed, CdSe/ZnS core−shell nanorods dispersed in a nematic phase display linearly polarized photoluminescence under an applied electric field.[1] To prevent the nanorods from aggregating, their concentration in the liquid is maintained below 100 mg dm^{-3}. The anisotropic orientation disappears upon removal of the electric field. Liquid crystalline (LC) polymers are considered powerful candidates for inducing nanorod orientation[33] because in the LC phase the nanorods can be aligned in a fixed orientation by super-cooling to a temperature below the glass transition temperature (T_g). In a previous trial,[33] most of the CdS nanorods were agglomerated rather than coaligned. Thus, we considered that alignment might be achieved by strengthening the molecular interactions between the nanorod surfaces and the nematic LC polymers.

In this paper, we demonstrate a simple and widely applicable method for unidirectionally aligning semiconductor nanorods on a substrate surface. Essentially, nematic LC-polymer-grafted nanorods are hybridized with small nematic LC molecules by surface-assisted hierarchical molecular ordering. Zinc oxide

Received: July 10, 2013
Accepted: December 3, 2013
Published: December 3, 2013

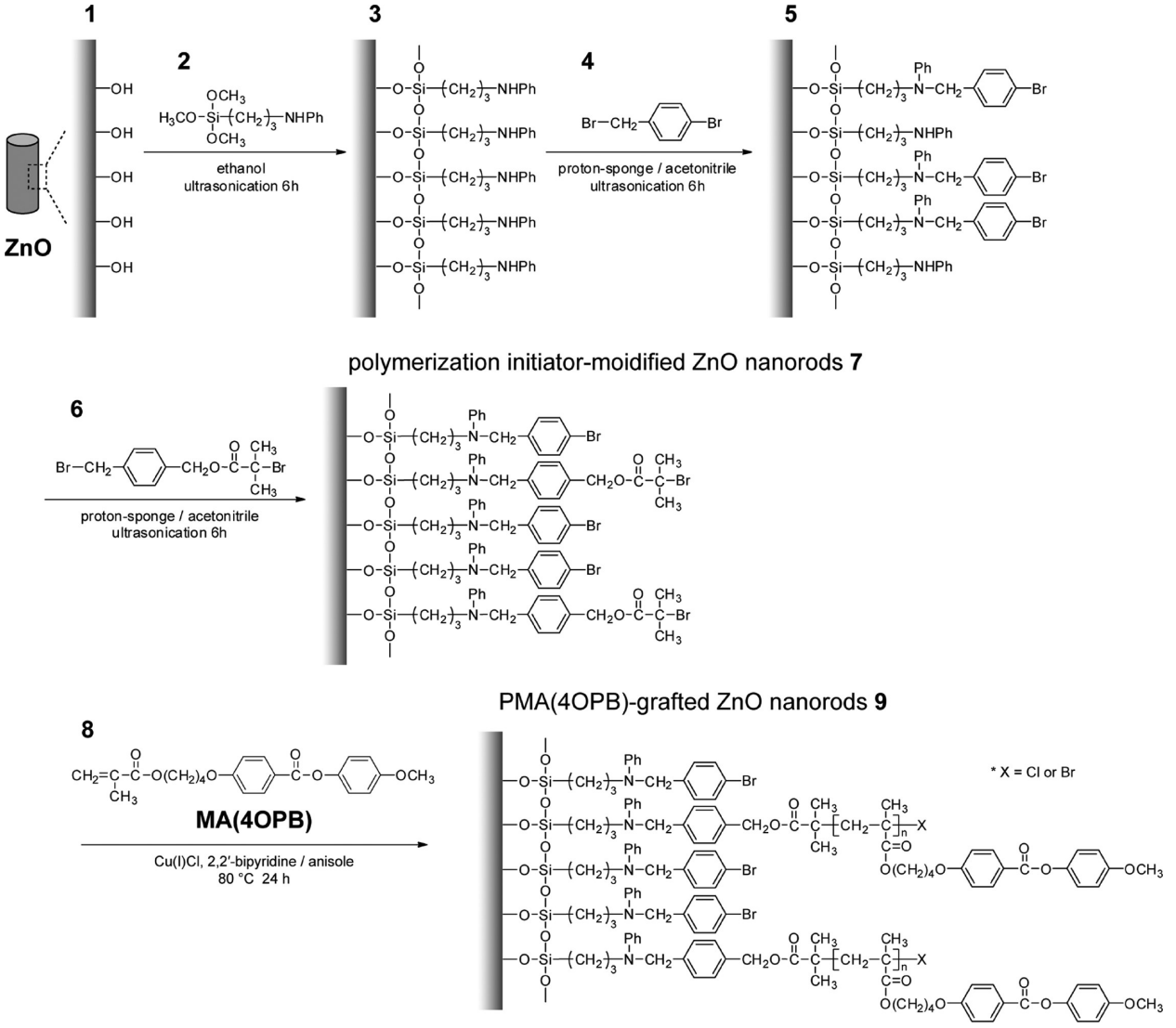

Figure 1. Schematic illustration of the preparation of ZnO nanorods modified with a capping agent (**4**), a controlled-density polymerization initiator (**6**), and a grafted nematic LC polymer PMA(4OPB).

(ZnO) semiconductor nanorods were selected for the study because their wide band gap makes them promising candidates for light-emitting devices in the ultraviolet (UV)-visible blue light region[34,35] and in nanoscale transistors.[4,5,36]

To achieve unidirectional nanorod orientation on the substrate, we adopt the following strategy: (i) induce homogeneous alignment of low viscosity nematic LC molecules onto a commercially available and commonly used rubbed polyimide alignment layer, (ii) induce homogeneous alignment of nematic LC polymers tethered to ZnO nanorods through cooperative molecular interactions between the nematic LC molecules and polymers, and (iii) orient the long axis of the ZnO nanorods in the rubbing direction of the polyimide alignment layer. The preparation of nematic LC-polymer-grafted ZnO nanorods from ZnO nanorods with density-regulated polymerization initiator moieties was essential for the success of step (iii).

2. EXPERIMENTAL SECTION

2.1. Materials. We adopted a poly{4-[4-(4-methoxyphenyloxycarbonyl)oxy]butyl methacrylate}, PMA(4OPB), showing a nematic liquid LC phase.[37] The PMA(4OPB)-grafted ZnO nanorods were prepared as illustrated in Figure 1. A typical procedure is described below.

Synthesis of N-Phenylamine-Modified ZnO Nanorods (3). ZnO nanorods **1** of average diameter 7 nm and length 50 nm were synthesized at a gram scale from zinc acetate in a basic ethanol solution, as we have previously reported.[38] The nanorods **1** (1.0 g) were dispersed in ethanol (100 mL) and sonicated for 6 h. Amounts of 1.0 g of *N*-(3-(trimethoxysilyl)propyl)aniline **2** (Tokyo Chemical Industry) and 0.30 g of hexylamine (Wako Pure Chemical) were added to the dispersion and reacted with sonication for 6 h, similar to the reaction with silica particles.[39] The obtained *N*-phenylamine-modified nanorods **3** were purified by centrifugation and redispersion in ethanol. Following centrifugation/redispersion the solvent was displaced into the acetonitrile.

Synthesis of Polymerization Initiator-Modified ZnO Nanorods (7). In the typical procedure, 54 mg of 4-bromobenzyl bromide **4** (Tokyo Chemical Industry) and 13.6 mg of proton sponge (Tokyo Chemical Industry) dissolved in 10 mL of acetonitrile were added to 40 mL of acetonitrile dispersion containing 0.62 g of **3**, which had been sonicated for 1 h. The mixture was sonicated for 6 h to obtain partially capped ZnO nanorods **5**. Following purification by centrifugation and redispersion, 40 mL of acetonitrile dispersion containing 0.51 g of **5** was mixed with 75 mg of benzyl 2-bromoisobutylate (BBnBiB) **6**[39] and 13.6 mg of proton sponge

dx.doi.org/10.1021/am404451z | ACS Appl. Mater. Interfaces 2014, 6, 811−818

dissolved in 10 mL of acetonitrile and sonicated for 6 h. The obtained nanorods modified with initiator moieties for atom transfer radical polymerization (ATRP) **7** were purified by centrifugation and redispersion. The modification densities of capping agents (d_{cap}) and ATRP initiator moieties (d_I) were determined by X-ray fluorescence (XRF) analysis.

*Synthesis of PMA(4OPB)-Grafted ZnO Nanorods (**9**).* A monomer 4-[4-(4-methoxyphenyloxycarbonyl)oxy]butylmethacrylate, MA-(4OPB) **8**, was synthesized as previously reported.[37] PMA(4OPB)-grafted nanorods were typically synthesized as follows: MA(4OPB) (192 mg) and 2,2′-bipyridine (Wako Pure Chemical) (9.4 mg) were dissolved in 1.75 mL of anisole. The solution was transferred to a 10 mL Schlenk tube and degassed through three cycles of vacuum with Ar replacement and added to 57 mg of ATRP initiator-modified nanorods **7** (d_I = 0.7 nm^{-2}) and Cu(I)Cl (Kanto Chemical) (3.0 mg). The mixture was stirred at room temperature for 5 min, sonicated for 10 min, and stirred at 80 °C for 24 h. Grafted nanorods were precipitated by adding methanol dropwise to the reaction solution and were collected by centrifugation. The grafted nanorods were washed in cycles of redispersion in chloroform, precipitation by methanol addition and centrifugation, and vacuum drying at 95 °C for 2 h. The weight fractions of organic components (w_{org}) in the polymer-grafted nanorods were determined from the feed ratio of ATRP initiator-modified nanorods to monomers and by monomer conversion estimated by ^{1}H NMR analysis.

The homopolymer PMA(4OPB) was similarly synthesized by ATRP using ethyl 2-bromoisobutyrate (Tokyo Chemical Industry) as an initiator instead of ATRP initiator-modified nanorods. The number-average molecular weight (M_n), weight-average molecular weight (M_w), and polydispersity (M_w/M_n) of the homopolymer were determined by gel permeation chromatography (GPC).

Synthesis of Smectic LC Polymer- And Amorphous Polymer-Grafted ZnO Nanorods. A smectic LC polymer poly[8-(4′-hexyloxybiphenyloxy)octyl methacrylate], PMA(8O6RB), and amorphous polymer poly(butyl methacrylate), PMA(Bu), were also grafted from **7** for comparison. The monomer 8-(4′-hexyloxybiphenyloxy)-octyl methacrylate, MA(8O6RB), was synthesized similar to PMA-(4OPB). PMA(8O6RB)-grafted nanorods were synthesized from ATRP in the same way as PMA(4OPB)-grafted nanorods using 233 mg of the monomer 8O6RB instead of MA(4OPB). PMA(Bu)-grafted nanorods were also synthesized using 192 mg of a butyl methacrylate monomer. Another homopolymer, PMA(8O6RB), was synthesized from the monomer MA(8O6RB) and ethyl 2-bromoisobutyrate as initiator.

2.2. Film Preparation. A low-molecular nematic liquid crystal 4′-(pentyloxy)-4-biphenylcarbonitrile (5OCB, Tokyo Chemical Industry) was added to an anisole dispersion containing 1.0 wt % grafted nanorods. The weight of 5OCB was adjusted to two, four, or eight times that of the dispersed grafted nanorods. The dispersion was passed through a membrane filter (pore diameter: 0.2 μm) and spin-coated onto a rubbed polyimide (JSR AL-1254) layer formed on a Si substrate. The sample was annealed at 63 °C for 12 h.

2.3. Instruments. XRF analysis was performed using an X-ray fluorescence spectrometer (RIGAKU ZSX Primus II). ^{1}H NMR spectra were obtained by an NMR spectrometer (Bruker Avance III; 400 MHz). GPC analysis was performed in a column (Shodex LF-804) equipped with an ultraviolet detector (JASCO UV-2075 plus) and a refractive index detector (Shodex RI101). The reference was a series of standard polystyrenes with tetrahydrofuran (THF) as eluent. Differential scanning calorimetry (DSC) was performed by an SII Exstar X-DSC7000 differential scanning calorimeter. The orientation of ZnO nanorods was observed by field emission scanning electron microscopy (FE-SEM, Hitachi S-4800) and analyzed by analysis software (Mitani WinROOF). The polymer-grafted nanorods were photo-oxidized by exposure to vacuum ultraviolet (VUV) light of wavelength 172 nm emitted from a Xe excimer lamp (USHIO UER20-172V) under a reduced pressure of 1.0 kPa for 1 h. Polarized absorption spectra were measured using a highly sensitive spectrophotometer (Bunko-keiki HSP-1).

3. RESULTS AND DISCUSSION

3.1. Controlling the Surface Density of ATRP Initiator Moieties. The modification density of ATRP initiator moieties was controlled by the stepwise modification scheme (Figure 1). The phenylamino moieties were partially deactivated by reacting the capping agent, 1-bromo-4-(bromomethyl)benzene (**4**), with **3**, yielding partially capped ZnO nanorods (**5**). ATRP initiator moieties were introduced to the residual phenylamino moieties by reacting **5** with **6**, yielding initiator-modified ZnO nanorods (**7**).

Table 1 shows the surface densities of the capping agents (d_{cap}/nm^{-2}) and the ATRP initiator moieties (d_I/nm^{-2}) obtained under three conditions. The *N*-phenylamine group was suitably deactivated by adjusting the feed ratio of *N*-phenylamine-modified nanorods to the capping agent. In this way, d_I could be precisely controlled between 0.3 and 2.0 nm^{-2}.

Table 1. Surface Densities of the Capping Agent and the ATRP Initiator Moiety

3 → 5		5 → 7	
[**4**]/[NHPh]$_0$[a]	d_{cap} (nm^{-2})	[**6**]/[NHPh]$_0$[b]	d_I (nm^{-2})
0	0	2.0	2.0
1.3	1.2	1.3	0.7
2.0	2.1	1.3	0.3

[a]Feed ratio of the concentration of the capping agent, [**4**], to the initial concentration of *N*-phenylamine moieties immobilized on **3**, [NHPh]$_0$. [b]Feed ratio of the concentration of BBnBiB, [**6**], to [NHPh]$_0$.

3.2. Liquid Crystalline Behaviors of PMA(4OPB)-Grafted Nanorods with 5OCB. The conditions under which PMA(4OPB)- and PMA(4OPB)-grafted ZnO nanorods **9** were synthesized by ATRP, and the characteristics of the synthesized nanorods, are shown in Table 2. PMA(4OPB) with a narrow polydispersity (M_w/M_n = 1.14) was obtained. A DSC curve of the PMA(4OPB) homopolymer is shown in Figure 2(b). The homopolymer shows a glass transition (T_g) at 51 °C and a phase transition at 104 °C, consistent with the previously reported PMA(4OPB) homopolymer prepared by free radical polymerization.[37] Polarization optical microscopy suggests that the phase transition at 104 °C is a nematic to isotropic phase transition. PMA(4OPB)-grafted ZnO nanorods were synthesized from ATRP initiator-modified nanorods at three different modification densities (d_I), namely, 0.7, 2.0, and 0.3 nm^{-2}.

We anticipated that the nanorods could be aligned by cooperative interaction of nematic LC polymer-grafted nanorods with small nematic LC molecules. Here, we investigate the LC behaviors of PMA(4OPB)-grafted nanorods mixed with 5OCB. Figure 2 shows DSC curves of 5OCB, homopolymer PMA(4OPB), PMA(4OPB)-grafted ZnO nanorods (d_I = 0.7 nm^{-2}), and three mixtures of PMA(4OPB)-grafted ZnO nanorods (d_I = 0.3, 0.7, and 2.0 nm^{-2}) in the presence of four-fold weight 5OCB. In the absence of 5OCB, the PMA(4OPB)-grafted ZnO nanorods showed a phase transition at 104 °C similar to the homopolymer (Figure 2(c)), which we interpret as a nematic phase. Similar thermal behaviors were observed in PMA(4OPB)-grafted nanorods of d_I = 2.0 and 0.3 nm^{-2}. The transition at 104 °C was not observed in PMA(4OPB)-grafted ZnO nanorods (d_I = 0.7 nm^{-2}) in the presence of 5OCB; instead, a single nematic-to-isotropic phase transition occurred at 68 °C, very close to the phase-transition temperature of pure 5OCB (Figure 2(d)). This single phase

Table 2. Synthetic Conditions[a] and Characterization of PMA(4OPB) and PMA(4OPB)-Grafted ZnO Nanorods Synthesized by ATRP

	$[M]_0/[I]_0$[b]	d_I (nm^{-2})	conversion (%)	w_{org} (−)	M_n	M_w/M_n	T_g (°C)	$T_{LC\text{-}Iso}$ (°C)
PMA(4OPB)	100	–	55	1.0	14 700	1.14	51	103
PMA(4OPB)-grafted nanorods	100[b]	0.7	42	0.62	–	–	53	106
	100[b]	2.0	17	0.66	–	–	53	105
	90[b]	0.3	50	0.44	–	–	55	104

[a][Initiator]:[Cu(I)Cl]:[bpy] = 1:6:12. The polymerization was carried out at 80 °C for 24 h. [b]Feed ratio of the initial monomer concentration $[M]_0$ to the initiator concentration $[I]_0$. T_g and $T_{LC\text{-}Iso}$ denote the glass transition and nematic-to-isotropic phase transition temperatures, respectively.

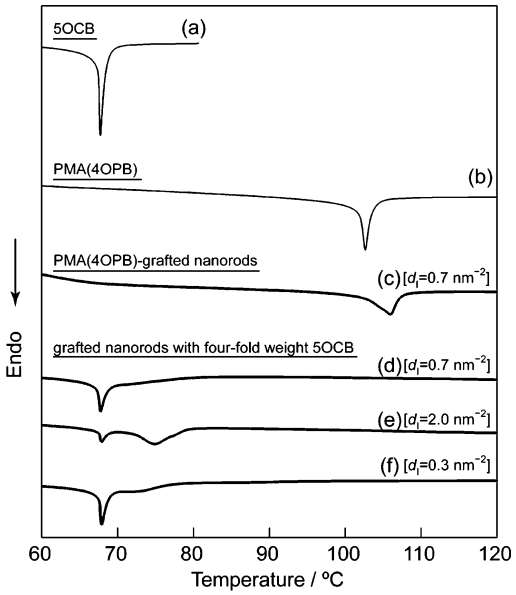

Figure 2. DSC curves of (a) 5OCB, (b) nematic LC homopolymer PMA(4OPB), (c) PMA(4OPB)-grafted ZnO nanorods, and (d–f) PMA(4OPB)-grafted nanorods mixed with four-fold weight 5OCB during the second heating process, conducted at 10 °C min^{-1}. [d_I, w_{org}] = [0.7 nm^{-2}, 0.62] (c, d), [2.0 nm^{-2}, 0.66] (e), and [0.3 nm^{-2}, 0.44] (f).

transition strongly suggests that 5OCB molecules are miscible in nematic PMA(4OPB) polymers tethered to the ZnO nanorod surface. The phase transition enthalpies (ΔH) of the PMA(4OPB)-grafted nanorods, expressed as total energy per molar quantity of LC mesogens, were 0.50 and 0.61 kJ mol^{-1} in the absence and presence of 5OCB, respectively. The phase transition enthalpy of 5OCB was 0.40 kJ mol^{-1}. Since ΔH increased in the presence of 5OCB, it appears that the PMA(4OPB)-grafted nanorods and 5OCB collectively contributed to the nematic-to-isotropic transition, without segregation.

By contrast, dense preparations of PMA(4OPB)-grafted ZnO nanorods (d_I = 2.0 nm^{-2}) mixed with 5OCB showed an additional broadened endothermic peak around 75 °C (Figure 2(e)). This peak indicates that densely packed and tethered PMA(4OPB) polymers were partially segregated from the 5OCB. Dense packing might prevent the mesogens of the grafted PMA(4OPB) polymers from interacting with homogenously aligned 5OCB on the rubbed polyimide film. Loosely packed PMA(4OPB)-grafted ZnO nanorods (d_I = 0.3 nm^{-2}) mixed with 5OCB showed an endothermic peak at 68 °C with a shoulder (Figure 2(f)). Although 5OCB is miscible in the loosely grafted nanorods, a minority of the grafted polymers might be unable to induce unidirectional nanorod orientation.

3.3. Orientation of Nematic LC Polymer-Grafted ZnO Nanorods.

Various dispersions of nematic LC polymer PMA(4OPB)-grafted ZnO nanorods were spin-coated and annealed at 63 °C for 12 h in an ambient atmosphere. The annealing was performed just below the nematic-to-isotropic phase transition. FE-SEM images of the resulting PMA(4OPB)-grafted ZnO nanorod films on the rubbed polyimide alignment layer are shown in Figure 3. The PMA(4OPB)-grafted ZnO nanorods were prepared from the initiator-modified nanorods 7 (d_I = 0.7 nm^{-2}). In the absence of 5OCB, the nanorod long axes were randomly oriented (Figure 3(a)). Interestingly, the nanorod long axes became aligned in the presence of 5OCB. As the weight ratio of 5OCB to the grafted nanorods was increased from two-fold (Figure 3(b)) to four-fold (Figure 3(c)) and from four-fold to eight-fold (Figure 3(d)), the ZnO nanorods became increasingly more aligned. The anisotropic orientations

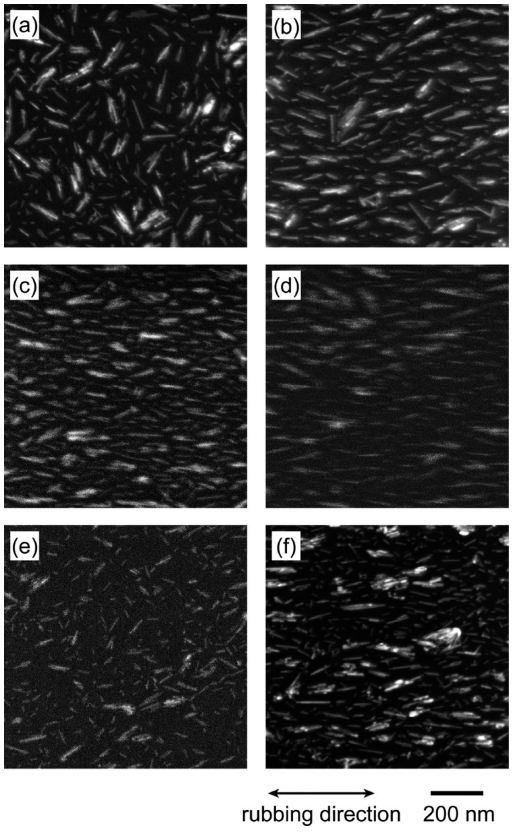

Figure 3. FE-SEM images of nematic LC PMA(4OPB)-grafted ZnO nanorods; [d_I, w_{org}] = [0.7 nm^{-2}, 0.62] (a–d), [2.0 nm^{-2}, 0.66] (e), and [0.3 nm^{-2}, 0.44] (f). The nanorods were spin-coated onto rubbed polyimide alignment layers (a) in the absence of 5OCB and with (b) two-fold weight 5OCB, (c, e, f) four-fold weight 5OCB, and (d) eight-fold weight 5OCB.

dx.doi.org/10.1021/am404451z | ACS Appl. Mater. Interfaces 2014, 6, 811–818

of the nanorod long axes were evaluated by plotting their angular distribution. The results are shown in Figure 4. Figure 4

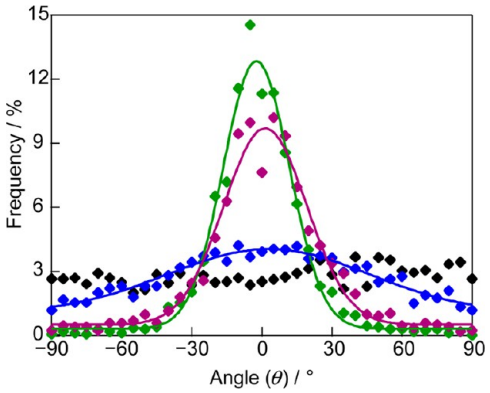

Figure 4. Angular distributions and fitted curves of the long-axis orientation angles of ZnO nanorods prepared in the absence of 5OCB (black) and with four-fold weight 5OCB (green, blue, and purple) on rubbed polyimide alignment layers; [d_I, w_{org}] = [0.7 nm^{-2}, 0.62] (black and green), [2.0 nm^{-2}, 0.66] (blue), and [0.3 nm^{-2}, 0.44] (purple). θ = 0° and θ = 90° signify that the long axis orients parallel and perpendicular, respectively, to the rubbing direction.

confirms that 5OCB encourages unidirectional parallel orientation of the PMA(4OPB)-grafted ZnO nanorods (green line). The parallel alignment of the nanorods on the polyimide layer depends on the surface density of the polymerization initiator moieties prepared from **7**. High surface density of the moieties (d_I = 2.0 nm^{-2}) resulted in random planar arrangement of the PMA(4OPB)-grafted nanorods (Figure 3(e); Figure 4, blue). PMA(4OPB)-grafted nanorods synthesized from moieties of low surface density (d_I = 0.3 nm^{-2}) formed nanorod aggregates, although isolated nanorods preferentially aligned in the rubbing direction (Figure 3(f); Figure 4, purple). Narrow angular distribution, i.e., unidirectional alignment, was obtained at the moiety surface density d_I = 0.7 nm^{-2} in the presence of four-fold weight 5OCB. The order parameter (S) of the nanorod long axis, calculated as $(1/2)\langle 3\cos^2\theta - 1\rangle$, was 0.85. Here, θ is the alignment angle of the long axis of the nanorods relative to the rubbing direction.

The results confirmed that moderate surface density of the polymerization initiator (around 0.7 nm^{-2}) was essential for unidirectional alignment of PMA(4OPB)-grafted ZnO nanorods on the polyimide alignment layer. Figure 5 illustrates a plausible mechanism for this alignment. The long axes of 5OCB molecules showing a nematic phase at 63 °C preferentially align in the rubbing direction. At moderate grafting density, polymer-grafted nanorods undergo strong interactions with the polymer-side-chain mesogens of the nematic LC 5OCB molecules. The molecular long axes of these mesogens orient along the long axes of the 5OCB molecules. Consequently, the long axes of the polymer-grafted ZnO nanorods hierarchically orient by attachment to the nematic polymers tethered to the ZnO surfaces. If the ZnO nanorods are modified with dense PMA(4OPB) polymers, the side-chain mesogens are largely prevented from interacting with the nematic LC 5OCB molecules, and the nematic polymers tether to the ZnO surfaces in random orientations. Supporting this idea, the thermal behaviors of PMA(4OPB)-grafted nanorods mixed with 5OCB suggest that cooperative and weak interactions occur when d_I = 0.7 nm^{-2} and d_I = 2.0 nm^{-2}, respectively. By

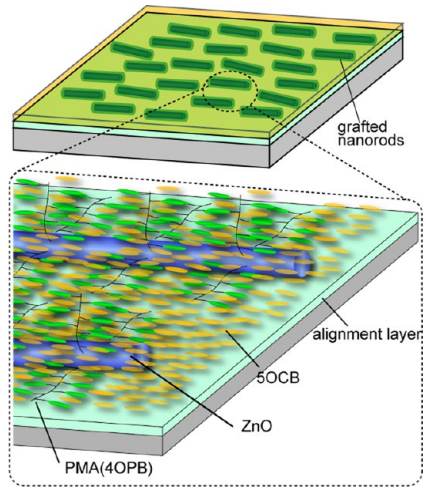

Figure 5. Schematic of the unidirectional orientation of nematic LC PMA(4OPB)-grafted ZnO nanorods in the presence of 5OCB assisted by a polyimide alignment layer.

contrast, ZnO nanorods modified with small quantities of PMA(4OPB) polymers are poorly dispersed in the 5OCB and instead tend to aggregate.

3.4. Anisotropic Optical Properties of Oriented ZnO Nanorods. The anisotropic absorption of the oriented nanorods could not be measured in the presence of tethered PMA(4OPB) and 5OCB because the absorption band of ZnO overlaps with that of the LC mesogens. For the optical measurements, a film of PMA(4OPB)-grafted nanorods (d_I = 0.7 nm^{-2}) with four-fold weight 5OCB was prepared on a rubbed polyimide alignment layer coated onto a silica substrate and exposed to VUV light (172 nm) to photo-oxidize the organic components. The nanorods remained aligned after the photo-oxidation (S = 0.82; Figure 6).

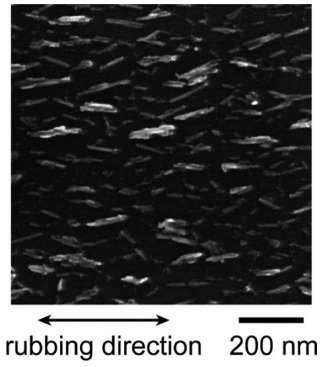

Figure 6. FE-SEM image of ZnO nanorods on a silica substrate, prepared by VUV exposure of PMA(4OPB)-grafted nanorods with four-fold weight 5OCB. The nanorods are unidirectionally orientated on the rubbed polyimide alignment layer. [d_I, w_{org}] = [0.7 nm^{-2}, 0.62].

Figure 7 shows polarized absorption spectra of ZnO nanorods prepared using PMA(4OPB)-grafted nanorods (d_I = 0.7 nm^{-2}) without 5OCB and with four-fold weight 5OCB. The spectra were collected by a probe light (diameter ~3 mm). In the absence of 5OCB, the nanorods prepared on the silica substrate are randomly oriented and therefore show isotropic absorption (Figure 7(a)). In contrast, anisotropic absorption by the nanorods is evident in the presence of 5OCB (Figure 7(b)). The dichroic ratio R, calculated as $A_{\parallel}/A_{\perp}$, was 3.1 at 360 nm,

dx.doi.org/10.1021/am404451z | ACS Appl. Mater. Interfaces 2014, 6, 811−818

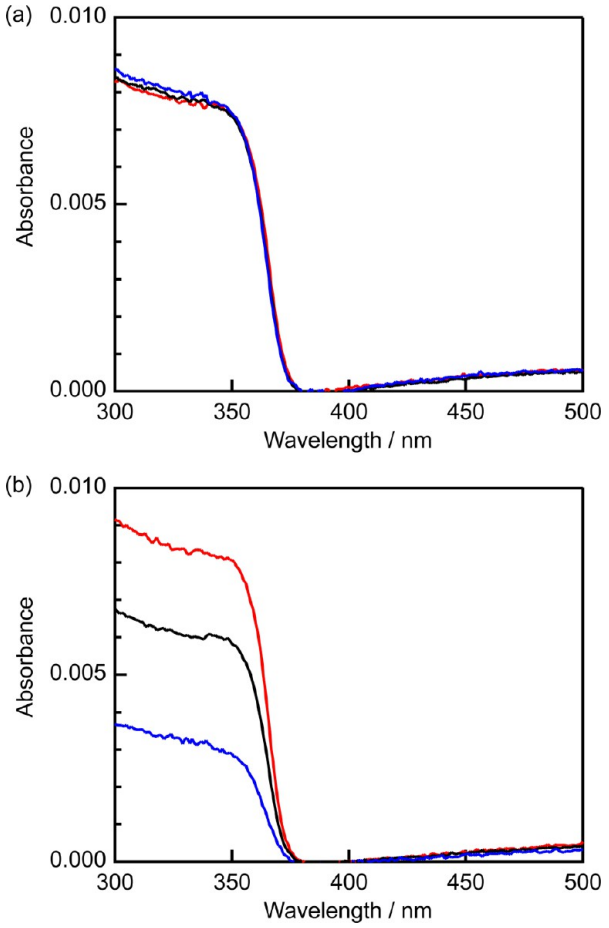

Figure 7. Polarized absorption spectra of ZnO nanorods prepared by annealing and photo-oxidation of PMA(4OPB)-grafted nanorods (a) without and (b) with four-fold weight 5OCB on rubbed polyimide alignment layers. [d_I, w_{org}] = [0.7 nm^{-2}, 0.62]. The spectra were collected using nonpolarized light (black) and light polarized parallel (red) and perpendicular (blue) to the rubbing direction.

where $A_{\parallel}$ and $A_{\perp}$ denote the measured absorbance of parallel and perpendicular incident light, respectively, relative to the rubbing direction. These optical properties strongly suggest that the PMA(4OPB)-grafted nanorods of d_I = 0.7 nm^{-2} in the presence of four-fold weight 5OCB encourage alignment of the ZnO nanorods on the substrate surfaces.

3.5. Liquid Crystalline Phases of Graft Polymers Affecting Orientation of ZnO Nanorods. To confirm whether nanorod alignment depends on the nematic LC polymers being tethered to the ZnO surfaces, we further investigated the surface-assisted orientation of ZnO nanorods (d_I = 0.7 nm^{-2}) modified with smectic LC methacrylate polymers: PMA(8O6RB) (with an 8-(4′-hexyloxybiphenyloxy)-octyl side chain) and amorphous methacrylate polymer, PMA(Bu) (with a butyl side chain). The conditions and characteristics of the synthesized nanorods are summarized in Table 3.

As was done for the PMA(4OPB)-grafted ZnO nanorods, 5OCB was mixed with the PMA(8OR6B)- and PMA(Bu)-grafted ZnO nanorods in a 4:1 weight ratio. The mixtures were spin-coated onto rubbed polyimide alignment layers and annealed at 63 °C for 12 h. The smectic LC PMA(8O6RB)-grafted ZnO nanorods showed evidence of dewetting. The nanorod long axes were randomly oriented regardless of the rubbing direction of the alignment layer (Figure 8(a)). The

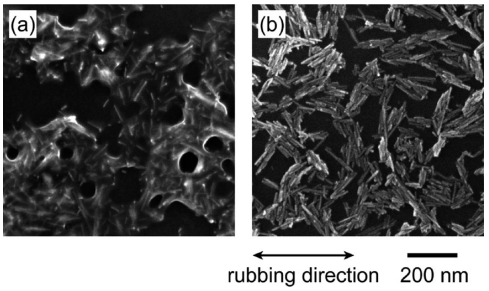

Figure 8. FE-SEM images of (a) smectic LC PMA(8O6RB)-grafted ZnO nanorods and (b) amorphous PMA(Bu)-grafted ZnO nanorods on rubbed polyimide alignment layers. The nanorods were mixed with four-fold weight 5OCB. [d_I, w_{org}] = [0.7 nm^{-2}, 0.59] (a) and [0.7 nm^{-2}, 0.52] (b).

PMA(8O6RB)-grafted ZnO nanorods underwent two endothermic phase transitions at 116 °C and 147 °C (Figure 9(c)). The thermal behaviors were almost identical to that of homopolymer PMA(8O6RB) (M_n = 24 500 g mol^{-2}, M_w/M_n = 1.11), with phase transitions at 118, 120, and 148 °C (Figure 9(b)). When mixed with 5OCB, the nanorods showed a nematic-to-isotropic phase transition attributable to pure 5OCB and a complicated 5OCB-associated phase transition between 120 °C and 140 °C (Figure 9(d)). These results suggest the exclusion of 5OCB molecules by strong intermolecular interactions among the smectic mesogens. The amorphous PMA(Bu)-grafted ZnO nanorods formed flakelike grains upon mixing with 5OCB, and their long axes were randomly oriented (Figure 8(b)). Thus, we confirmed that nematic LC polymers tethered to ZnO nanorods are necessary for surface-assisted nanorod alignment in the presence of nematic 5OCB molecules.

4. CONCLUSION

In summary, two factors were essential for alignment of ZnO nanorods on a rubbed polyimide alignment layer using the liquid crystal alignment technique. First, the polymers tethered

Table 3. Synthetic Conditions[a] and Characterization of PMA(8O6RB) and PMA(8O6RB)-Grafted ZnO Nanorods Synthesized by ATRP

	$[M]_0/[I]_0$[b]	d_I (nm^{-2})	conversion (%)	w_{org} (-)	M_n	M_w/M_n	T_g (°C)	transition temperature (°C)		
PMA(8O6RB)	100	–	49	1.0	24500	1.11	–	118	120	148
PMA(8O6RB)-grafted nanorod	100[b]	0.7	31	0.59	–	–	–	116		147
PMA(Bu)-grafted nanorod	100[b]	0.7	74	0.52	–	–	29			

[a][Initiator]:[Cu(I)Cl]:[bpy] = 1:6:12. The polymerization was carried out at 80 °C for 24 h. [b]Feed ratio of the initial monomer concentration $[M]_0$ to the initial initiator concentration $[I]_0$.

dx.doi.org/10.1021/am404451z | ACS Appl. Mater. Interfaces 2014, 6, 811−818

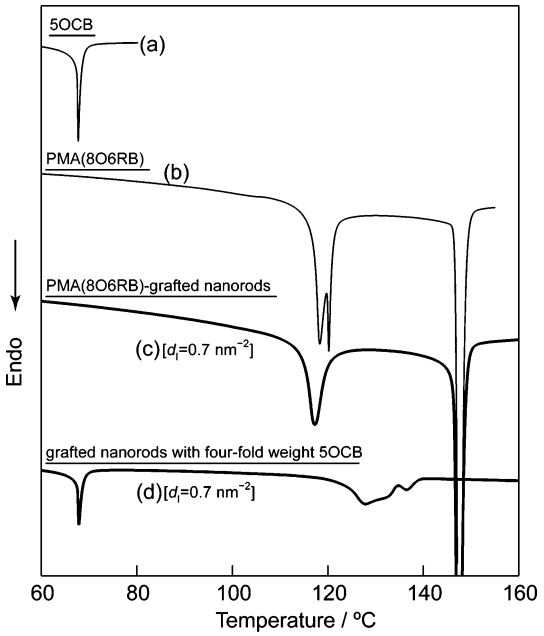

Figure 9. DSC curves of (a) 5OCB, (b) smectic LC homopolymer PMA(8O6RB), (c) PMA(8O6RB)-grafted ZnO nanorods, and (d) PMA(8O6RB)-grafted nanorods mixed with four-fold weight 5OCB during the second heating process, conducted at 10 °C min^{-1}. [d_l, w_{org}] = [0.7 nm^{-2}, 0.59].

to the inorganic nanorod surfaces should show a nematic phase together with small nematic liquid crystalline 5OCB molecules. Second, to enable sufficient interaction of 5OCB with the polymer, the grafted polymers should be moderately dense. Under these conditions, the mixtures harmoniously behave as an organic–inorganic hybrid material, cooperating to favor homogeneous alignment on the rubbed polyimide alignment layer. Therefore, the unidirectional orientation of isolated inorganic nanorods was achieved by a bottom-up nanotechnology using a conventional LC alignment technique.

■ ASSOCIATED CONTENT

Supporting Information

Transmission electron microscope image and size distribution of PMA(4OPB)-grafted ZnO nanorods (d_l = 0.7 nm^{-2}). This material is available free of charge via the Internet at http://pubs.acs.org.

■ AUTHOR INFORMATION

Corresponding Author

*E-mail: skubo@tagen.tohoku.ac.jp.

Notes

The authors declare no competing financial interest.

■ ACKNOWLEDGMENTS

This work was supported in part by KAKENHI (21850004) Grant-in-Aid for Research Activity Start-up and Management Expenses Grants for National Universities Corporations from the Ministry of Education, Culture, Sports, Science and Technology of Japan (MEXT). The authors are also grateful to Dr. K. Hayashida (Toyota Central R&D Labs.) for his assistance in synthesizing *p*-(bromomethyl)benzyl 2-bromoisobutyrate and the surface modification of ZnO nanorods. The authors are also grateful to Professors H. Fujikake and T. Ishinabe (Tohoku University) and Professors A. Shishido and J. Mamiya (Tokyo Institute of Technology) for their assistance in preparing polyimide alignment layers. The authors are also grateful to Prof. A. Muramatsu, K. Kanie, and M. Nakaya (Tohoku University) for their help in the XRF analysis.

■ REFERENCES

(1) Mukhina, M. V.; Danilov, V. V.; Orlova, A. O.; Fedorov, M. V.; Artemyev, M. V.; Baranov, A. V. *Nanotechnology* **2012**, *23*, 325201.
(2) Carbone, L.; Nobile, C.; De Giorgi, M.; Sala, F. D.; Morello, G.; Pompa, P.; Hytch, M.; Snoeck, E.; Fiore, A.; Franchini, I. R.; Nadasan, M.; Silvestre, A. F.; Chiodo, L.; Kudera, S.; Cingolani, R.; Krahne, R.; Manna, L. *Nano Lett.* **2007**, *7*, 2942–2950.
(3) Hu, J.; Li, L.-s.; Yang, W.; Manna, L.; Wang, L.-w.; Alivisatos, A. P. *Science* **2001**, *292*, 2060–2063.
(4) Park, W. I.; Kim, J. S.; Yi, G.-C.; Bae, M. H.; Lee, H. J. *Appl. Phys. Lett.* **2004**, *85*, 5052–5054.
(5) Kim, H.-J.; Lee, C.-H.; Kim, D.-W.; Yi, G.-C. *Nanotechnology* **2006**, *17*, S327–S331.
(6) He, G.-n.; Huang, B.; Shen, H. *Nanotechnology* **2011**, *22*, 065304.
(7) Park, W.; Yi, G. C. *Adv. Mater.* **2004**, *16*, 87–90.
(8) Singh, D.; Narasimulu, A. A.; Garcia-Gancedo, L.; Fu, Y. Q.; Hasan, T.; Lin, S. S.; Geng, J.; Shao, G.; Luo, J. K. *J. Mater. Chem. C* **2013**, *1*, 2525–2528.
(9) Fragalà, M. E.; Aleeva, Y.; Malandrino, G. *Thin Solid Films* **2011**, *519*, 7694–7701.
(10) Yang, L. L.; Zhao, Q. X.; Willander, M. *J. Alloys Compd.* **2009**, *469*, 623–629.
(11) Chen, H.-G.; Lian, H.-D.; Hung, S.-P.; Wang, C.-F. *J. Cryst. Growth* **2013**, *362*, 231–234.
(12) Park, W. I.; Kim, D. H.; Jung, S. W.; Yi, G.-C. *Appl. Phys. Lett.* **2002**, *80*, 4232–4234.
(13) Yu, D.; Hu, L.; Li, J.; Hu, H.; Zhang, H.; Zhao, Z.; Fu, Q. *Mater. Lett.* **2008**, *62*, 4063–4065.
(14) Dev, A.; Panda, S. K.; Kar, S.; Chakrabarti, S.; Chaudhuri, S. *J. Phys. Chem. B* **2006**, *110*, 14266–14272.
(15) Zhou, H.; Fallert, J.; Sartor, J.; Dietz, R. J. B.; Klingshirn, C.; Kalt, H.; Weissenberger, D.; Gerthsen, D.; Zeng, H.; Cai, W. *Appl. Phys. Lett.* **2008**, *92*, 132112.
(16) Zhang, X. X.; Liu, D. F.; Zhang, L. H.; Li, W. L.; Gao, M.; Ma, W. J.; Ren, Y.; Zeng, Q. S.; Niu, Z. Q.; Zhou, W. Y.; Xie, S. S. *J. Mater. Chem.* **2009**, *19*, 962–969.
(17) Feng, Q. J.; Shen, D. Z.; Zhang, J. Y.; Liang, H. W.; Zhao, D. X.; Lu, Y. M.; Fan, X. W. *J. Cryst. Growth* **2005**, *285*, 561–565.
(18) Liu, B.; Aydil, E. S. *J. Am. Chem. Soc.* **2009**, *131*, 3985–3990.
(19) Kim, W.-S.; Jang, Y.-G.; Kim, D.-H.; Kim, H.-C.; Hong, S.-H. *CrystEngComm* **2012**, *14*, 4963–4966.
(20) Miao, W.; Zhu, M. M.; Li, Z. C.; Zhang, Z. J. *Mater. Trans.* **2008**, *49*, 2288–2291.
(21) Ma, Y.; Liu, F.; Zhu, M.; Yin, P. *Thin Solid Films* **2009**, *517*, 3492–3495.
(22) Harnack, O.; Pacholski, C.; Weller, H.; Yasuda, A.; Wessels, J. M. *Nano Lett.* **2003**, *3*, 1097–1101.
(23) Hu, Z.; Fischbein, M. D.; Querner, C.; Drndic, M. *Nano Lett.* **2006**, *6*, 2585–2591.
(24) Nobile, C.; Fonoberov, V. A.; Kudera, S.; DellaTorre, A.; Ruffino, A.; Chilla, G.; Kipp, T.; Heitmann, D.; Manna, L.; Cingolani, R.; Balandin, A. A.; Krahne, R. *Nano Lett.* **2007**, *7*, 476–479.
(25) Zorn, M.; Tahir, M. N.; Bergmann, B.; Tremel, W.; Grigoriadis, C.; Floudas, G.; Zentel, R. *Macromol. Rapid Commun.* **2010**, *31*, 1101–1107.
(26) Zanella, M.; Gomes, R.; Povia, M.; Giannini, C.; Zhang, Y.; Riskin, A.; Van Bael, M.; Hens, Z.; Manna, L. *Adv. Mater.* **2011**, *23*, 2205–2209.
(27) Concetta, N.; Luigi, C.; Angela, F.; Roberto, C.; Liberato, M.; Roman, K. *J. Phys.: Condens. Matter* **2009**, *21*, 264013.
(28) Sun, B.; Sirringhaus, H. *J. Am. Chem. Soc.* **2006**, *128*, 16231–16237.
(29) Li, L. S.; Alivisatos, A. P. *Adv. Mater.* **2003**, *15*, 408–411.

(30) Ploshnik, E.; Salant, A.; Banin, U.; Shenhar, R. *Adv. Mater.* **2010**, *22*, 2774−2779.
(31) Kanie, K.; Sugimoto, T. *J. Am. Chem. Soc.* **2003**, *125*, 10518−10519.
(32) Kanie, K.; Muramatsu, A. *J. Am. Chem. Soc.* **2005**, *127*, 11578−11579.
(33) Ezhov, A. A.; Shandryuk, G. A.; Bondarenko, G. N.; Merekalov, A. S.; Abramchuk, S. S.; Shatalova, A. M.; Manna, P.; Zubarev, E. R.; Talroze, R. V. *Langmuir* **2011**, *27*, 13353−13360.
(34) Chandrinou, C.; Boukos, N.; Stogios, C.; Travlos, A. *Microelectron. J.* **2009**, *40*, 296−298.
(35) Chen, Y. W.; Qiao, Q.; Liu, Y. C.; Yang, G. L. *J. Phys. Chem. C* **2009**, *113*, 7497−7502.
(36) Wang, X.; Zhou, J.; Song, J.; Liu, J.; Xu, N.; Wang, Z. L. *Nano Lett.* **2006**, *6*, 2768−2772.
(37) Schoenhals, A.; Wolff, D.; Springer, J. *Polym. Adv. Technol.* **1996**, *7*, 853−857.
(38) Kubo, S.; Nakagawa, M. *Chem. Lett.* **2012**, *41*, 1137−1138.
(39) Hayashida, K.; Tanaka, H.; Watanabe, O. *Polymer* **2009**, *50*, 6228−6234.